Published in final edited form as:
J Oral Maxillofac Surg. 2011 June ; 69(6): e50–e57. doi:10.1016/j.joms.2010.12.049.

OSTEOCHONDRAL INTERFACE REGENERATION OF THE RABBIT MANDIBULAR CONDYLE WITH BIOACTIVE SIGNAL GRADIENTS

Nathan H. Dormer, B.S.[1], **Kamal Busaidy, B.D.S., F.D.S.R.C.S.**[2], **Cory J. Berkland, Ph.D.**[1,3,4], and **Michael S. Detamore, Ph.D.**[1,4]

[1] Bioengineering Program, University of Kansas, Lawrence, KS 66045

[2] Department of Oral and Maxillofacial Surgery, University of Texas Health Science Center, Houston, TX, 77030

[3] Department of Pharmaceutical Chemistry, University of Kansas, Lawrence, KS, 66045

[4] Department of Chemical & Petroleum Engineering, Lawrence, KS, 66045

Abstract

PURPOSE—Tissue engineering solutions focused on the temporomandibular joint (TMJ) have expanded in number and variety over the past decade to address the treatment of TMJ disorders. The existing literature on approaches for healing small defects in the TMJ condylar cartilage and subchondral bone, however, is sparse. The purpose of this study was thus to evaluate the performance of a novel gradient-based scaffolding approach to regenerate osteochondral defects in the rabbit mandibular condyle.

MATERIALS AND METHODS—Miniature bioactive plugs for regeneration of small mandibular condylar defects in New Zealand White rabbits were fabricated. The plugs were constructed from poly(D,L-lactic-co-glycolic acid) (PLGA) microspheres with a gradient transition between cartilage-promoting and bone-promoting growth factors.

RESULTS—At six weeks of healing, results suggested that the implants provided support for the neo-synthesized tissue as evidenced by histology and 9.4T magnetic resonance imaging.

CONCLUSION—The inclusion of bioactive factors in a gradient-based scaffolding design is a promising new treatment strategy for focal defect repair in the TMJ.

Keywords

TMJ; Osteochondral; Interface; Gradient; Microsphere; PLGA; BMP-2; TGF-β_1

INTRODUCTION

As the field of osteochondral tissue engineering advances, it is critical that researchers consider a wide range of bone and cartilage interfaces. One of the lesser-investigated osteochondral interfaces is that of the TMJ. Damage to the TMJ disc or condyle from trauma

Corresponding Author: Michael S. Detamore, Ph.D., University of Kansas, Department of Chemical and Petroleum Engineering, 1530 W 15th Street, 4132 Learned Hall, Lawrence, KS 66045, Phone: (785) 864-4943, Fax: (785) 864-4967, detamore@ku.edu.

or arthritic conditions can induce a lifetime of pain and restricted jaw motion for patients, even in daily activities such as talking, eating, and yawning. Thus, development of tissue regeneration solutions that either focus on the disc or condyle have the potential to impact the lives of many. Primary contributions to the mandibular condyle tissue engineering literature are currently limited to a handful of investigations with a wide array of materials and regenerative solutions.

Strategies for producing patient-specific condyle-shaped scaffolds based on computed tomography and/or magnetic resonance images have been developed by Hollister and colleagues.[1] Employing solid free-form fabrication (SFF), the group has produced cylindrical osteochondral constructs[2, 3] and condyle/ramus-shaped bone constructs.[4] *In vivo* studies in mice demonstrated substantial bone ingrowth and glycosaminoglycan (GAG) formation.[2–5] Later, a TMJ reconstruction study was performed using a selective laser sintering (SLS) method to fabricate a poly(caprolactone) (PCL) condyle/ramus scaffold for implantation into the TMJs of Yucatan minipigs.[6] The condylar heads of the scaffolds were packed with autologous iliac crest bone marrow. Compared to controls, there was an increase in regenerated bone volume, and there was evidence of cartilage-like tissue as well at three months.

Mao's group[7–9] has utilized poly(ethylene glycol) diacrylate (PEG-DA) hydrogels with encapsulated marrow-derived mesenchymal stem cells to create stratified bone and cartilage layers resembling a human condyle. After 12 weeks of subcutaneous implantation, collagen I and bone-specific proteins were localized in the osteogenic layer and collagen II and glycosaminoglycans were present in the chondrogenic layer.[9]

Our group has taken an entirely different approach, focusing on the relevance of cell source *in vitro*. In one series of studies, porcine mandibular condylar cartilage cells were compared to porcine chondrocytes from ankle cartilage in both monolayer[10] and on three-dimensional (3D) scaffolds.[11] In monolayer, the condylar cartilage cells experienced a faster growth rate but the hyaline cartilage cells produced more extracellular matrix. On PGA scaffolds,[11] the condylar cartilage cells were outperformed in matrix synthesis once again, with hyaline cartilage cells producing more collagen II relative to collagen I. An earlier study demonstrated that human umbilical cord mesenchymal stromal cells divided also much faster and produce significantly more matrix than porcine condylar cartilage cells.[12] Thus the possibility of autologous transplantation of cartilage cells may also be a solution for TMJ tissue engineering.

Beyond the three aforementioned groups, an assortment of different approaches have been employed, most of which were *in vivo* studies using histology and/or imaging to validate engineered constructs.[13–17] A recent investigation[18] even demonstrated that low-intensity pulsed ultrasound (LIPUS) can improve the integration of full tissue-engineered mandibular condyles *in vitro* and *in vivo*. Moreover, whether it be full condyle replacement with SFF or hydrogels, or investigation of promising cellular candidates for scaffold seeding, TMJ tissue engineering has been a burgeoning field. Approaches focusing on tissue regeneration in small mandibular defects, however, have seldom been investigated. This is an important issue, as there might not always be a need for full condyle/ramus tissue replacement (e.g., for filling a defect after coring out a mandibular osteophyte).

While bone morphogenetic protein (BMP)-2-loaded PLGA has been used as biomaterial for full condyle replacement in rabbits,[19] in the present study, microsphere-based PLGA scaffolds were used for small TMJ condylar defects, a method based on previous *in vitro* reports.[20–22] Bone and cartilage regeneration in TMJ condyles of New Zealand White rabbits was evaluated using scaffolds with a continuous transition from cartilage-promoting,

(transforming growth factor (TGF)-β_1-loaded microspheres) to bone-promoting (BMP-2-loaded microspheres) regions. The induced defect size was approximately 1.0 mm in diameter and 3.0 mm in depth, the maximum achievable size as to not fracture the condyle and underlying condylar neck. Regeneration was evaluated at six weeks with magnetic resonance imaging (MRI) and histological staining. Our goal was to determine whether our continuously-graded design would facilitate osteochondral defect regeneration in the rabbit mandibular condyle.

MATERIALS AND METHODS

Materials

PLGA (50:50 lactic acid:glycolic acid, acid end group, M_W ~40,000 Da) of intrinsic viscosity (i.v.) 0.33 dL/g was purchased from Lakeshore Biomaterials (Birmingham, AL). Poly(vinyl alcohol) (PVA; 88% hydrolyzed, 25,000 Da) was obtained from Polysciences, Inc. (Warrington, PA). TGF-β_1 and BMP-2 were purchased from Peprotech, Inc. (Rocky Hill, NJ). Six adult New Zealand White rabbits were obtained from Myrtle's Rabbitry (Thompsons Station, TN).

Preparation of Protein-loaded Microspheres

BMP-2 was reconstituted in 10 mg/mL bovine serum albumin (BSA) in phosphate buffered saline (PBS) (both from Sigma Aldrich, St. Louis, MO). TGF-β_1 was reconstituted in 1 mg/mL BSA in PBS. The reconstituted protein solutions were individually mixed with PLGA dissolved in dichloromethane (DCM) (20% w/v) at a loading ratio of 30 ng TGF-β_1 or 60 ng BMP-2 per 1.0 mg of PLGA. The final mixture was then sonicated over ice (50% amplitude, 20 seconds). Using PLGA-protein emulsions, uniform protein-loaded PLGA microspheres were prepared using technology from our previous reports.[22–25] Briefly, using acoustic excitation produced by an ultrasonic transducer, regular jet instabilities were created in the polymer stream that produced uniform polymer droplets. An annular carrier non-solvent stream (0.5% w/v PVA in DI H_2O) surrounding the droplets was produced using a nozzle coaxial to the needle. The emanated polymer/carrier streams flowed into a beaker containing the non-solvent. Incipient polymer droplets were stirred for 3–4 hours to allow solvent evaporation, which were then filtered and rinsed with DI H_2O to remove residual PVA, and stored at −20 °C (Fig. 1a). Blank control microspheres were prepared in a similar manner, where the protein solution was replaced with an equivalent volume of BSA solution (1 mg/mL). Microspheres with a nominal diameter of approximately 70 μm were produced as a result. Following 48 hours of lyophilization, the size distribution of microsphere preparations was determined using a Coulter Multisizer 3 (Beckman Coulter Inc., Fullerton, CA) equipped with a 560-μm aperture.

Scaffold Fabrication

Gradient scaffolds were prepared using a technology reported previously.[22, 24, 25] Briefly, lyophilized protein-loaded microspheres were dispersed in DI H_2O 2.5% w/v, and separately loaded into two syringes. Each construct in total contained ~4 mg of microspheres. The suspensions were pumped into a cylindrical glass mold (1.0 mm diameter, 3.0 cm in height) in a controlled manner using programmable syringe pumps (PHD Ultra, Harvard Apparatus, Inc., Holliston, MA). Using a filter (particle retention > 3 μm) at the bottom of the mold, DI H_2O was filtered, while the microparticles stacked in the mold until a height of 3.0 mm was reached. The profile for gradient constructs was linear, where the transition region from TGF- β_1 to BMP-2 constituted the second quarter of the scaffold volume, and the top quarter and bottom half contained all TGF-β_1- or BMP-2-loaded microspheres, respectively (Fig. 1b). Using an additional infusion syringe pump and a vacuum pump, a constant level of distilled water was maintained in the mold. The stacked microspheres were then sintered

using a 100% ethanol treatment for 1 hour.[22] Each gradient scaffold contained, in total, approximately 20 ng of TGF-β_1 and 66 ng of BMP-2. The molds (containing the scaffolds) were freeze-dried for 48 hours, then the gradient scaffolds were retrieved and stored at −20 °C. Blank scaffolds were prepared in a similar manner. Prior to surgical implantation, scaffolds were sterilized with ethylene oxide for 12 hours.

Description of Experimental Groups

Three different treatment groups were investigated: (i) Group S: sham surgeries, in which a defect was made, but no implant was placed, (ii) Group B: blank scaffolds with no growth factors encapsulated, and (iii) Group G: gradient scaffolds with a transition between BMP-2- and TGF-β_1-loaded microspheres (Fig. 1c). Assignment of treatment groups for each TMJ of each rabbit was randomly determined at the beginning of the study, so that only the corresponding implant was thawed at the time of surgery (Table 1.).

Surgical Procedure

The study received approval from the Animal Welfare Committee of the University of Texas, Health Science Center at Houston. Following stable general anesthesia, hair was shaved from area around each TMJ. A Frost stitch was placed to secure the eyelids, and the surgical area was disinfected with a Nolvasan surgical scrub (Chlorhexidine Diacetate). The rabbit was then draped in sterile fashion. Only strict aseptic techniques and sterile instruments were used. Local anesthetic was infiltrated into the soft tissues overlying the joint (0.25 ml Lidocaine HCl with 1:100000 epinephrine). The TMJ was surgically exposed using a horizontal incision 1 cm in length, beginning 2 cm posterior to the lateral canthus and extending directly posteriorly. Sharp and blunt dissection was performed through subcutaneous tissue and fascia until the lateral aspect of the TMJ capsule was reached. A #15 blade was used to gain access to the inferior joint space, exposing the head of the condyle. Care was taken to not scuff the cartilaginous cap on the condyle. Defects were created using a #701 fissure bur (approximately 1.0 mm diameter, 3.0 mm depth). The defect was placed in the anterior region of the superior surface of the condyle, the widest part of the articular surface (Fig. 2a). Defects were then filled by press-fitting one of two engineered plugs (Fig. 2b), either blank or gradient, into the defect (Groups B and G). Care was taken during scaffold packaging prior to sterilization to maintain orientation for implantation. In Group S, no scaffold was placed. The joint was then washed of debris, and the wound closed in two layers using resorbable sutures. Following wound closure of the first TMJ, a similar procedure was performed on the contralateral TMJ according to the pre-assigned treatment group. After both procedures were finished, rabbits were administered 0.01 mg/kg buprenorphine subcutaneously and returned to their cages. All rabbits received a regular diet post-operatively, and a 5-day course of Enrofloxacin and Penicillin. Each rabbit's condition was monitored during anesthesia, surgery, and post-op care by appropriate veterinary staff.

Magnetic Resonance Imaging

At six weeks post-operatively, rabbits were sacrificed and the TMJs and surrounding tissues were retrieved en bloc. Further dissection was conducted in the laboratory to isolate the mandibular condyles. The samples were placed in 10% neutral buffered formalin (Fisher Scientific, Pittsburgh, PA) for at least three days. After fixation, the condyles were rinsed and mounted in cell culture grade agarose (Sigma Aldrich) for MRI. T2-weighted imaging over the central 2.0 mm of the TMJ condylar surface was done in a 9.4 T Varian system. Slices were taken every 400 μm. After imaging, the samples were rinsed and placed back in 10% neutral buffered formalin prior to histological processing. MRI scans were qualitatively evaluated using MRIcron software (Georgia State University/Georgia Tech Center for advanced Brain Imaging). A representative number of scans were taken from each

experimental group by persons knowledgeable of the treatments, but histological processing and rating was performed by a blinded team member.

Histological Staining

Samples were rinsed and dehydrated in graded alcohol. Before plastic embedding, the samples were infiltrated for four days with a solution consisting of 85 v/v% methylmethacrylate, 14 v/v% dibutylphthalate, 1 v/v% poly(ethylene glycol) 400, and 7 mg/mL benzoyl peroxide (BPO) (all reagents from Sigma Aldrich). The infiltrate was changed every 24 hours. Following infiltration, condyles were embedded in 20 mL glass scintillation vials with a solution identical to the infiltrate, with the exception of using 4 mg/mL BPO and an additional 33 μL of N,N-dimethyl-p-toluidine (reagents from Sigma). The vials were kept at 4 °C for one week to polymerize. After polymerization, the glass vials were broken and samples removed.

Following plastic embedding, the samples were cut into blocks with a Buehler Isomet 1000 precision saw (Lake Bluff, IL). Care was taken to locate the center of the condyle/ramus (where defects were induced), and sectioning was performed into this region for 400 μm. Sectioning was done on a Microm HM 355S microtome using a tungsten carbide blade with a sample thickness of 10 μm, placed on gelatin-coated slides, and dried for 48 hours at 44 °C (materials from Fisher Scientific). After drying, plastic resin was removed from the slides using a series of 2-methoxyethylacetate (20 minutes, three times), acetone (5 minutes, two times), and DI H_2O (5 minutes, two times). Safranin-O/Fast Green staining for GAGs, Alizarin Red staining for calcium deposition, and von Kossa staining for calcium phosphate was done as described elsewhere.[26] Slides were then dehydrated in graded alcohol and cleared in xylene for mounting (materials from Sigma Aldrich).

Sample Scoring

To evaluate results of this pilot study, a simple scoring system (Table 2) was developed to evaluate cartilage and bone regeneration separately, where points were assigned for new tissue growth across the diameter of the original defect, and throughout the depth of the original defect. The assignment of histological scores was aided by qualitatively evaluating T2 relaxation images and staining intensity for GAGs, calcium ions, and calcium phosphate. The defect area was rated in comparison to the adjacent native tissue. Morphological features in histological sections were matched as closely as possible to MRI images in each sample, as histological sections could not correspond to the *exact* location of MRI slices, but only represent the same region.

Statistical Analyses

Statistical analyses between blank and gradient groups at six weeks were performed using a single factor analysis of variance (ANOVA) in SPSS/PASW 18.0 software (SPSS Incorporated, Chicago, IL), followed by a Tukey's Honestly Significant Difference *post hoc* test when significance was detected below the $p = 0.05$ value. All quantitative results were expressed as the mean ± standard deviation.

RESULTS

Post-surgical Course

Post-operatively, none of the rabbits exhibited any adverse events at the surgical site. All were able to maintain adequate food intake to maintain baseline weight. One rabbit had transient conjunctivitis that responded to Tobramycin ophthalmic drops, and one developed a corneal ulcer. Both of these complications were related to the liberal use of surgical skin

preparation, which managed to get into the eye. Rabbits with complications are also noted in Table 1. All rabbits survived until being sacrificed.

Cartilage Regeneration

MRI scans indicated distinct differences between treatment groups with respect to cartilage regeneration (Fig. 3). Articular surfaces in sham and blank treatments were variable, with some samples exhibiting a disorganized fibrocartilage ingrowth, and others a nearly continuous layer of neo-cartilage tissue. Conversely, MRI scans of gradient treatments showed consistent regeneration of a smooth condylar surface. Upon histological staining for GAGs and rating of all samples however, the variability of healing in blank constructs proved to be wider than previously indicated in MRI imaging alone. There were no statistically significant differences in cartilage healing among treatments, but the difference between blank and gradient groups had the lowest p-value among all statistical comparisons ($p = 0.156$) (Table 3).

Bone Formation

Alizarin Red and von Kossa staining for calcium deposition and calcium phosphate presence indicated only subtle differences in patterns of mineralization (Fig. 4). While subchondral trabeculae appeared thicker in gradient groups compared to blank treatments, the apposition did not necessarily reach the underside of the cartilage layer in half of the gradient samples. With the histological scoring system accounting for both apposition depth and breadth, there were no statistically significant differences in cumulative ratings among groups (Table 3). Bony regions in MRI scans were complimentary to histological staining in all samples.

DISCUSSION

From MRI and GAG staining, it appeared that growth factor incorporation in the gradient group showed little advantage for total volume of cartilage regeneration compared to the sham treatment at six weeks. Conversely, the presence of a scaffold in gradient groups did not negatively inhibit cartilage formation, and the new cartilage layers in gradient treatments were smoother than in sham samples. This suggested that having a scaffold might have provided mechanical support for the defect as new tissue formed. It is also important to note that in human disease states, where this application is targeted, cartilage tissue would not regenerate spontaneously. Thus, the physiological relevance of the sham performance might be limited. In addition, blank treatments had noticeably thinner cartilage layers, which may have been due to a lack of bioactive stimuli in neo-cartilage synthesis. To verify the behavior of the gradient implant in disease states, future studies will require the implant to be tested in an animal model with degenerative joint disease.

Although there were no statistically significant differences in new bone formation and mineral deposition between groups, the average histological rating was slightly higher in gradient samples than in blank and sham treatments. As noted, the difference in ratings was most likely due to overall thicker trabeculae in gradient groups, possibly from growth factor incorporation. In addition, the subchondral bone layers in gradient and blank groups were more uniform across the underside of the cartilage layer than in sham treatments, another possible testament to the advantages of having the mechanical support of a scaffolding material. While it could be argued that a higher BMP-2 concentration in gradient groups might lend to more complete bone apposition, the variance in gradient samples suggests that BMP-2 presence, in this particular size defect, may have less of an impact on bone growth than other factors such as mechanical loading.

From the data presented in the current study, the concept of repairing small osteochondral mandibular condylar defects with gradients of bioactive signaling has been proven feasible, although some design variables need to be investigated. The physical support of a scaffold might have been advantageous in promoting smooth subchondral bone and articular surfaces. There was also evidence that TGF-β_1 inclusion in the scaffold promoted thicker cartilage regeneration. Conversely, with such small diameter defects, the volume of bone apposition may not be greatly influenced by BMP-2 incorporation after six weeks of healing. To demonstrate the benefits of the gradient design in TMJ defects, future studies should include greater sample numbers in larger animal models for shorter and longer periods of time. In addition, increased defect sizes in larger animals would more accurately simulate physiological conditions in humans. Lastly, while there have been a myriad of stratified (layered) osteochondral tissue engineering solutions,[27] this approach used a continuous gradient to transition between cartilage- and bone-regenerating regions. The relevance of a gradient, versus a flat transition between growth factors, should also be addressed in future *in vivo* studies.

CONCLUSION

Studies to date for mandibular condyle tissue engineering have demonstrated the ability to apply different strategies to create shape-specific scaffolds, have explored different cell sources, and have looked at various bioactive signaling strategies. This study, for the first time, investigated small osteochondral defects in rabbit mandibular condyles that were treated with microsphere-based scaffolds with a gradient of bioactive signaling. In addition to establishing feasibility, the results suggest that there may be distinct advantages to the gradient design, such as more uniform neo-tissue synthesis than in unfilled defects, and thicker cartilage layers than were achieved in scaffolds devoid of growth factors. The current study focused on a small defect based on the constraints of the dimensions of the rabbit condyle, although we emphasize that the technology is highly versatile, with the scaffold being tailored in its dimensions and gradient profile to larger defects in larger animals and humans. Moreover, we have demonstrated the ability to create shape-specific scaffolds with our microsphere-based approach,[28] and thus the approach from the current study may hold promise in evolving from defect regeneration to replacement of the entire osteochondral mandibular condyle.

Acknowledgments

The authors would like to express their gratitude to the Oral and Maxillofacial Surgery Foundation, the Arthritis Foundation, the National Institutes of Health (NIH/NIDCR 1 R21 DE017673-01), to the NIGMS/NIH Pharmaceutical Aspects of Biotechnology Training grant (T32-GM008359) for supporting N. H. Dormer, and to Drs. Sang-Pil Lee and William Brooks at The University of Kansas Medical Center Hoglund Brain Imaging Facility for assistance with MRI.

References

1. Hollister SJ, Levy RA, Chu TM, et al. An image-based approach for designing and manufacturing craniofacial scaffolds. Int J Oral Maxillofac Surg. 2000; 29:67. [PubMed: 10691148]
2. Schek RM, Taboas JM, Segvich SJ, et al. Engineered osteochondral grafts using biphasic composite solid free-form fabricated scaffolds. Tissue Eng. 2004; 10:1376. [PubMed: 15588398]
3. Schek RM, Taboas JM, Hollister SJ, Krebsbach PH. Tissue engineering osteochondral implants for temporomandibular joint repair. Orthod Craniofac Res. 2005; 8:313. [PubMed: 16238612]
4. Williams JM, Adewunmi A, Schek RM, et al. Bone tissue engineering using polycaprolactone scaffolds fabricated via selective laser sintering. Biomaterials. 2005; 26:4817. [PubMed: 15763261]
5. Hollister SJ, Lin CY, Saito E, et al. Engineering craniofacial scaffolds. Orthod Craniofac Res. 2005; 8:162. [PubMed: 16022718]

6. Smith MH, Flanagan CL, Kemppainen JM, et al. Computed tomography-based tissue-engineered scaffolds in craniomaxillofacial surgery. Int J Med Robot. 2007; 3:207. [PubMed: 17631675]
7. Alhadlaq A, Mao JJ. Tissue-engineered neogenesis of human-shaped mandibular condyle from rat mesenchymal stem cells. J Dent Res. 2003; 82:951. [PubMed: 14630893]
8. Alhadlaq A, Elisseeff JH, Hong L, et al. Adult stem cell driven genesis of human-shaped articular condyle. Ann Biomed Eng. 2004; 32:911. [PubMed: 15298429]
9. Alhadlaq A, Mao JJ. Tissue-engineered osteochondral constructs in the shape of an articular condyle. J Bone Joint Surg Am. 2005; 87:936. [PubMed: 15866954]
10. Wang L, Detamore MS. Effects of growth factors and glucosamine on porcine mandibular condylar cartilage cells and hyaline cartilage cells for tissue engineering applications. Arch Oral Biol. 2009; 54:1. [PubMed: 18640663]
11. Wang L, Lazebnik M, Detamore MS. Hyaline cartilage cells outperform mandibular condylar cartilage cells in a tmj fibrocartilage tissue engineering application. Osteoarthritis Cartilage. 2009; 17:346. [PubMed: 18760638]
12. Bailey MM, Wang L, Bode CJ, et al. A comparison of human umbilical cord matrix stem cells and temporomandibular joint condylar chondrocytes for tissue engineering temporomandibular joint condylar cartilage. Tissue Eng. 2007; 13:2003. [PubMed: 17518722]
13. Chen F, Mao T, Tao K, et al. Bone graft in the shape of human mandibular condyle reconstruction via seeding marrow-derived osteoblasts into porous coral in a nude mice model. J Oral Maxillofac Surg. 2002; 60:1155. [PubMed: 12378491]
14. Chen F, Chen S, Tao K, et al. Marrow-derived osteoblasts seeded into porous natural coral to prefabricate a vascularised bone graft in the shape of a human mandibular ramus: Experimental study in rabbits. Br J Oral Maxillofac Surg. 2004; 42:532. [PubMed: 15544883]
15. Weng Y, Cao Y, Silva CA, et al. Tissue-engineered composites of bone and cartilage for mandible condylar reconstruction. J Oral Maxillofac Surg. 2001; 59:185. [PubMed: 11213987]
16. Abukawa H, Terai H, Hannouche D, et al. Formation of a mandibular condyle in vitro by tissue engineering. J Oral Maxillofac Surg. 2003; 61:94. [PubMed: 12524615]
17. Srouji S, Rachmiel A, Blumenfeld I, Livne E. Mandibular defect repair by tgf-beta and igf-1 released from a biodegradable osteoconductive hydrogel. J Craniomaxillofac Surg. 2005; 33:79. [PubMed: 15804584]
18. El-Bialy T, Uludag H, Jomha N. In vivo ultrasound-assisted tissue-engineered mandibular condyle: A pilot study in rabbits. Tissue Engineering Part C: Methods. 2010 EPub ahead of print.
19. Ueki K, Takazakura D, Marukawa K, et al. The use of polylactic acid/polyglycolic acid copolymer and gelatin sponge complex containing human recombinant bone morphogenetic protein-2 following condylectomy in rabbits. J Craniomaxillofac Surg. 2003; 31:107. [PubMed: 12628601]
20. Dormer NH, Singh M, Wang L, et al. Osteochondral interface tissue engineering using macroscopic gradients of bioactive signals. Annals of Biomedical Engineering - Special Issue on Interfacial Bioengineering. 2010; 38:2167.
21. Singh M, Dormer N, Salash J. Three-dimensional macroscopic scaffolds with a gradient in stiffness for functional regeneration of interfacial tissues. Journal of Biomedical Materials Research - Part A. 2010; 94:870. [PubMed: 20336753]
22. Singh M, Morris CP, Ellis RJ, et al. Microsphere-based seamless scaffolds containing macroscopic gradients of encapsulated factors for tissue engineering. Tissue Engineering Part C: Methods. 2008; 14:299. [PubMed: 18795865]
23. Berkland C, Kim K, Pack DW. Fabrication of plg microspheres with precisely controlled and monodisperse size distributions. Journal of Controlled Release. 2001; 73:59. [PubMed: 11337060]
24. Dormer NH, Singh M, Wang L, et al. Osteochondral interface tissue engineering using macroscopic gradients of bioactive signals. Annals of biomedical engineering. 2010
25. Singh M, Dormer N, Salash J. Three-dimensional macroscopic scaffolds with a gradient in stiffness for functional regeneration of interfacial tissues. Journal of Biomedical …. 2010
26. An, Y.; Martin, K. Handbook of histology methods for bone and cartilage. Humana Press; 2003.
27. Dormer N, Berkland C, Detamore M. Emerging techniques in stratified designs and continuous gradients for tissue engineering of interfaces. Annals of Biomedical Engineering - Special Issue on Interfacial Bioengineering. 2010; 38:2121.

28. Singh M, Sandhu B, Scurto A, et al. Microsphere-based scaffolds for cartilage tissue engineering: Using subcritical co2 as a sintering agent. Acta Biomaterialia. 2010; 6:137. [PubMed: 19660579]

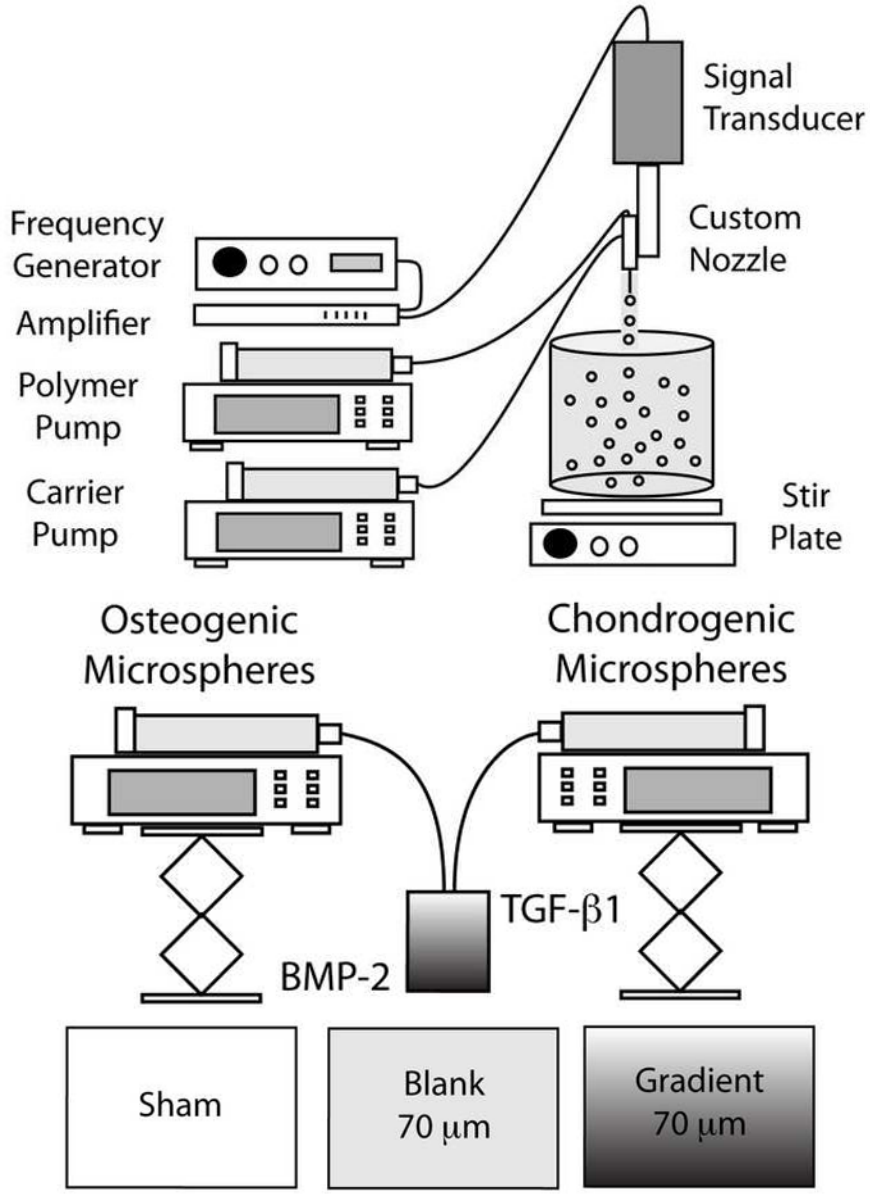

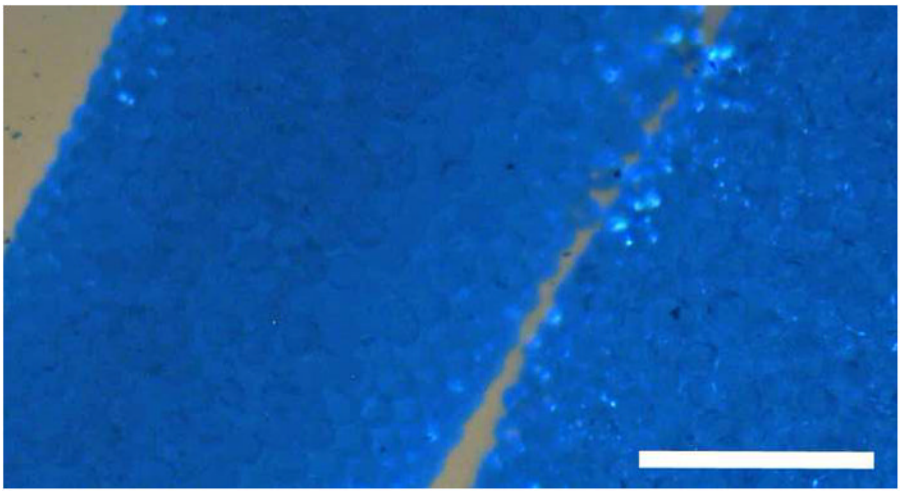

Figure 1.

Microsphere and scaffold fabrication process. (A) Microspheres were made from a polymer stream (20% w/v PLGA in DCM) and annular carrier stream (0.5% w/v PVA in DI H_2O) with an ultrasonic transducer; (B) Programmable pumps created a gradient in microsphere types; (C) Experimental groups for each time point (six rabbits at twelve weeks). Sham surgeries were performed with no implant, blank groups contained microspheres with no growth factor, gradient groups contained a gradient of BMP-2 and TGF-β_1; (D) Microscope image of microsphere-based scaffold with particles of 70 μm. Scale bar = 500 μm.

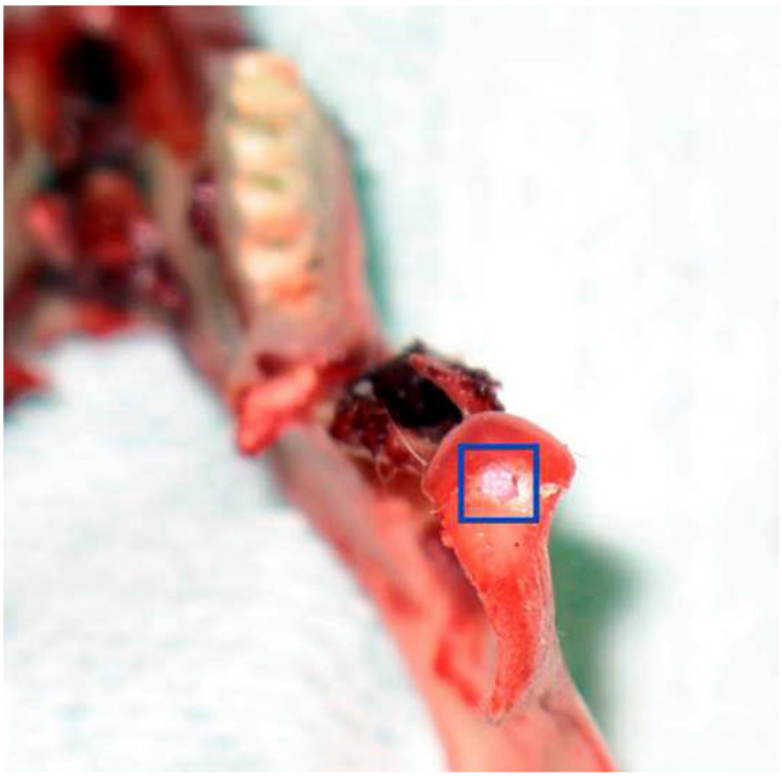

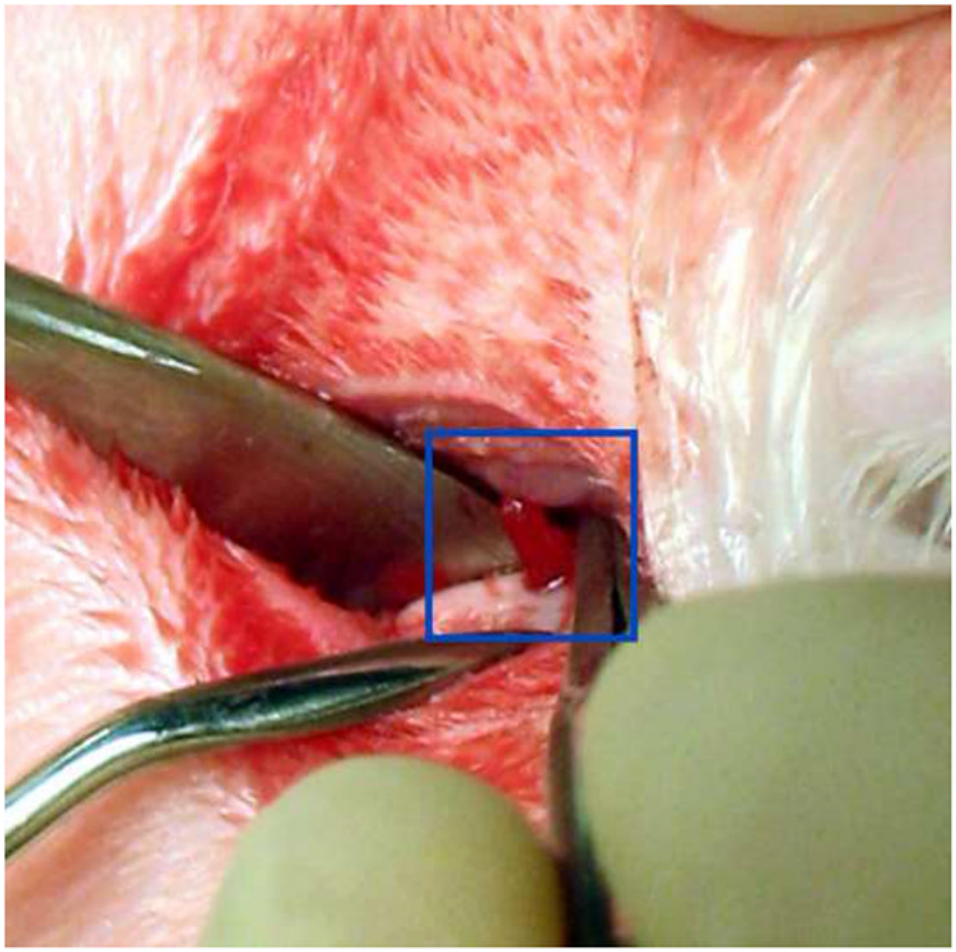

Figure 2.
Implant placement. (A) The defect was created in the anterior region of the TMJ condyle, as seen in this excised mandible specimen; (B) Implant being press fitted into articulating surface of TMJ condyle..

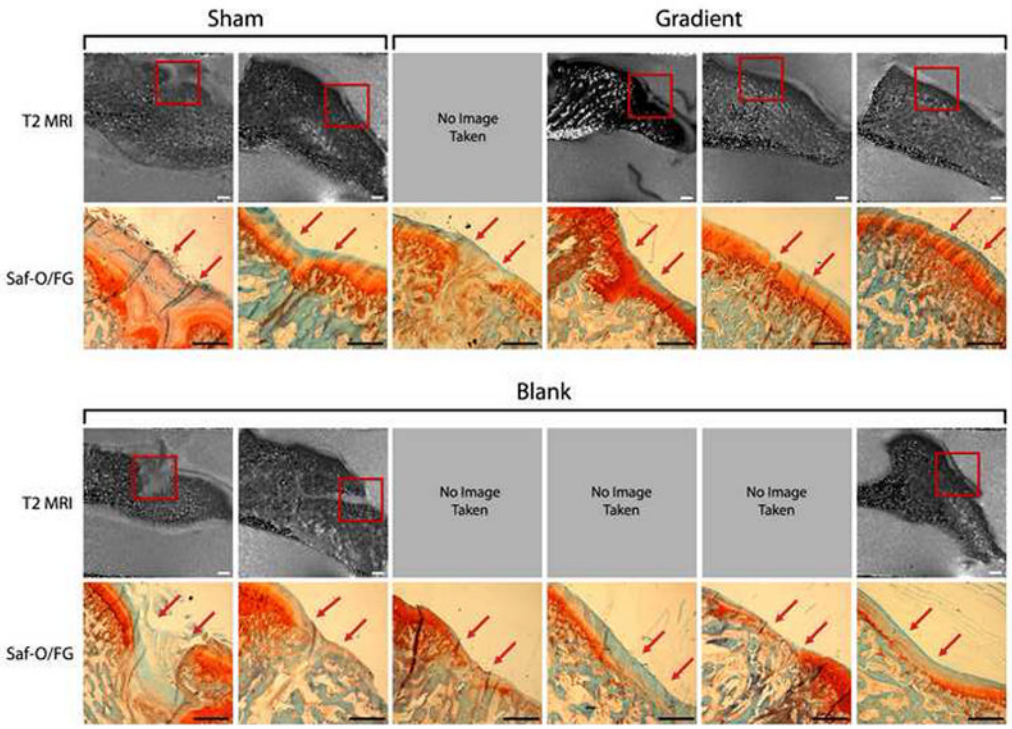

Figure 3.

Cartilage Evaluation - T2 MRI images and histological staining of rabbit TMJs at six weeks of time for sham, blank, gradient groups. “SF” denotes Safranin-O/Fast Green for GAGs. Sham and gradient samples earned similar histological scores for cartilage thickness width over defects, whereas blank samples had noticeably thinner neo-cartilage compared to gradient samples, although this was not statistically significant ($p = 0.156$). Red arrows mark the approximate edges of the original defect. Scale bar = 1.0 mm in MRI and histological images.

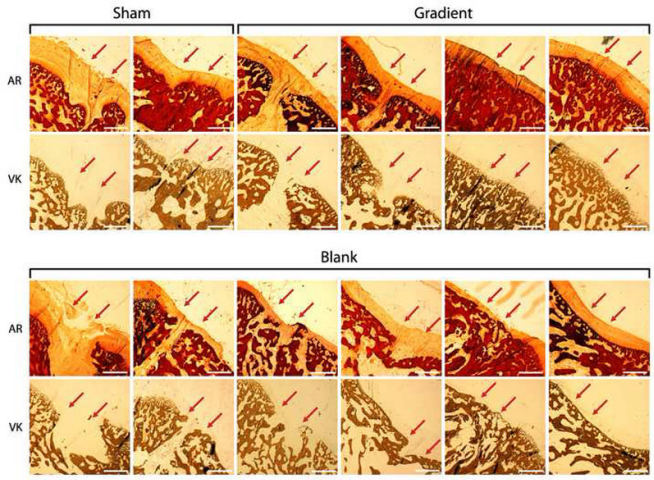

Figure 4.

Bone Evaluation - histological staining of rabbit TMJs at six weeks for sham, blank, and gradient groups. “AR” denotes Alizarin Red for calcium ions, and “VK” denotes von Kossa for calcium phosphate. There was a slight tendency for subchondral trabeculae in gradient samples to be thicker. Samples are arranged in the exact same order as seen in Figure 3. Red arrows mark the approximate edges of the original defect. Scale bar = 1.0 mm.

Table 1

Assignment of treatment groups for each condyle.

	Treatment	
Animal	**Left**	**Right**
Rabbit 1*	G	B
Rabbit 2*	B	S
Rabbit 3	G	B
Rabbit 4	B	S
Rabbit 5	G	B
Rabbit 6	G	B

*Noted ophthalmic complications.

Table 2

Histological scoring used for rating cartilage and bone.

Cartilage Scorecard	Bone Scorecard
Closure Across Diameter	**Apposition Across Diameter**
No closure (1)	No apposition (1)
25% Closed (2)	25% Apposition (2)
50% Closed (3)	50% Apposition (3)
75% Closed (4)	75% Apposition (4)
Full closure (5)	Full Apposition (5)
Thickness of Cartilage	**Apposition Toward Surface**
No Thickness (1)	No apposition (1)
25% Thickness (2)	25% Apposition (2)
50% Thickness (3)	50% Apposition (3)
75% Thickness (4)	75% Apposition (4)
Full Thickness (5)	Full Apposition (5)
Total Possible = 10	***Total Possible = 10***

Table 3

Histogical scoring results at six weeks.

	Healing at 6 Weeks	
Group (*n*)	**Cartil age**	**Bone**
Sham (2)	9.5 ± 0.7	7.0 ± 2.8
Blank (6)	6.8 ± 2.3	7.3 ± 2.7
Gradient (4)	9.3 ± 1.0	7.5 ± 3.3